

## High density physics in Reversed Field Pinches: comparison with Tokamaks and Stellarators

M.E. Puiatti, P.Scarin, G. Spizzo, M. Valisa, M. Agostini, A. Alfier, A. Canton, L. Carraro, R.Paccagnella, I. Predebon, R. Lorenzini, D. Terranova, D. Bonfiglio, S. Cappello, R.Cavazzana, S. Dal Bello, E. Gazza, P. Innocente, L. Marrelli, R. Piovan, F. Sattin, P. Zanca

*Consorzio RFX, Associazione Euratom-ENEA sulla Fusione, Padova, Italy*

e-mail contact of main author: mariaester.puiatti@igi.cnr.it

**Abstract.** Reversed Field Pinches (RFPs) share with Tokamaks and Stellarators the experimental evidence of an upper limit for the maximum value of the electron density at which they can operate. Above a certain density level, well described by the Greenwald law for Tokamaks and RFPs, a radiative collapse with strong plasma cooling is observed, predominantly due to processes occurring at the plasma boundary. In the RFX-mod RFP close to the density limit a radiating belt, poloidally symmetric and toroidally localized, develops in the region where the plasma is shrunk as an effect of the  $m=0$  tearing modes. The phenomenology recalls that of MARFES or plasma detachment, though, unlike Tokamaks, the appearance of the radiating belt is associated to a soft landing of the plasma discharge.

The paper reports the experimental pattern of the RFX-mod plasmas close to the density limit, including density and radiation profiles, plasma flow and turbulence. Particles are toroidally conveyed towards the region of maximum shrinking of the plasma column where they accumulate. The interpretation is related to the topology of MHD  $m=0$  and  $m=1$  modes: the reconstruction of the magnetic topology shows that the highly radiating region corresponds to the presence of peripheral  $m=0$  magnetic islands well detached from the wall. The emerging indication is that in RFPs a reduction of the  $m=0$  activity could be a way to overcome the density limit.

### 1. INTRODUCTION

Both an upper and a lower operational limit for density are found in all the major magnetic configuration devices. The upper one is more critical, because the performance of a future reactor depends on the product  $n_e^2 \cdot f(T)$ , with  $f(T)$  function of the plasma temperature.

The occurrence of a high density limit in experiments characterized by different magnetic configurations raises the question if the mechanism behind it is regulated by a common physics. Tokamak and Reversed Field Pinches (RFP) share the same limit: the maximum average density at which each device can operate is bound to the plasma current, according to the so-called Greenwald law:  $n \leq n_G = I_p / \pi a^2$  ( $10^{20} \text{ m}^{-3}$ , MA) [1]. A number of studies have been carried out to explain the nature of this empirical limit. In most of them it has been related to the occurrence of a thermal edge instability, with increasing radiation and edge plasma cooling, often acting in synergy with recycling or edge turbulence [see for example 1,2,3,4,5,6]. An exception is represented by the case of the TEXT Tokamak [7], where the limit was related to a micro-turbulence induced transport effect. However, in general, for both Tokamaks and RFPs, the origin of the Greenwald limit is believed to be a thermal instability that, due to the interplay between perpendicular and parallel transport, develops at the plasma edge. In Tokamaks the consequent shrinking of the current profile can often trigger a plasma disruption. Conversely, the density limit in RFPs leads to a soft landing of the plasma discharge rather than to a fast termination. In Tokamaks, improved core transport as well as fuelling via pellets or strong neutral beam heating may lead beyond the Greenwald threshold [8]. This indirectly strengthens the idea that the limit originates from processes occurring at the edge.

Stellarators experience a high density limit too [2,9], well described by the Sudo scaling [10], allowing an operating density range wider than in Tokamaks and RFPs and accompanied by thermal and radiative instabilities. In Stellarators, the limit mainly depends on the heating

power and magnetic field strength and it is attributed to a central impurity accumulation with consequent temperature collapse or to a detachment process induced by impurity radiation. However, the impact on plasma equilibrium is less strong than in Tokamaks, and therefore the discharge does not disrupt. Indeed, a peculiar feature in the case of Stellarators is that the temperature collapse can recover, resulting in radiation oscillations and plasma jumping in and out from a state of equilibrium (the so-called ‘breathing’ discharge, [2]).

This paper gives a complete experimental pattern of the high density discharges in the RFP device RFX-mod, discussing the common aspects and the peculiar features of the RFP when compared to the other magnetic configurations.

## 2. EXPERIMENTAL FINDINGS

### 2.1 General phenomenology

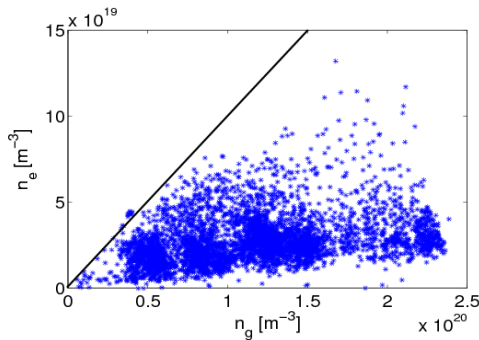


Fig.1: Greenwald plot for RFX-mod

In the RFP device RFX-mod ( $R=2\text{m}$ ,  $a=0.459\text{m}$ ) the improved control of the magnetic boundary [11], based on a system of 192 feedback controlled saddle coils, allowed the avoidance of the severe plasma-wall interaction (PWI) phenomena that in the previous device RFX at high density led to carbon blooming and fast termination of the plasma discharge [12]. Yet, the maximum density is still limited to the Greenwald value, as shown in fig.1, where plasma currents from 0.4 to 1.5 MA are included. At high density the database is still limited for the highest currents. One reason is that

in RFX-mod the best performance is obtained in the Quasi Single Helicity (QSH) regime, where the MHD spectrum is dominated by a single  $m=1$ ,  $n=-7$  mode [13]. Presently, QSH are spontaneously obtained at high current for densities well below the Greenwald limit. However, even in Multiple Helicity (MH) regimes, where a large spectrum of  $m=1$  modes resonates inside the  $q=0$  surface, an objective difficulty has been found in sustaining high densities at high current. As the plasma density in RFX-mod is basically sustained by the graphite wall recycling, this difficulty could be ascribed to a wall conditioning/fuelling problem rather than to a more strict density limit at high current.

Independently of the plasma current, when the density increases approaching the Greenwald value, due to plasma cooling and resistivity increase the toroidal flux decreases, resulting in a shrinking of the current profile and soft decrease of the plasma current.

As already reported for RFX [12], due to the deformation of the Last Close Flux Surface (LCFS) induced by the MHD  $m=1$  mode coherent superposition (LM, Locked Modes), the PWI is not toroidally symmetric, and this can be an important factor in determining the plasma behaviour at high density. It has to be mentioned that the non-linear interaction between the  $m=1$  modes generates an  $m=0$  perturbation, as the coherent phase relation between  $m=1$  modes propagates to the  $m=0$  too. On RFX-mod the LM has been put into rotation according to a scheme dubbed Virtual Shell + Rotating Perturbation [14]. This offers the practical advantage of dragging the LM (and consequently the  $m=0$  perturbation) all around the torus, allowing the plasma to be diagnosed by all the diagnostic systems placed at different toroidal positions.

### 2.2 Radiation pattern

For a plasma discharge at  $n/n_G=0.8$ , Fig. 2b shows a toroidal section of the whole 3D total

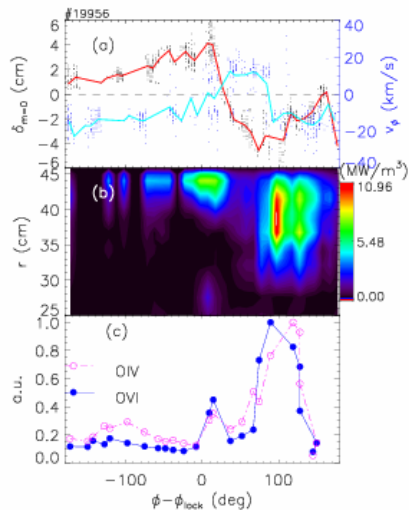


Fig.2 As a function of the toroidal angle: (a) local displacement  $\delta^0$  (red) and flow (blue) (b) total radiation (c) OIV and OVI emissivities

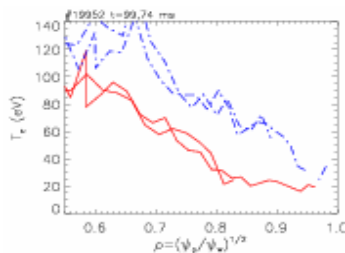


Fig. 3: edge radial profile of  $T_e$  corresponding with (red) and w/o (blue) radiating belts

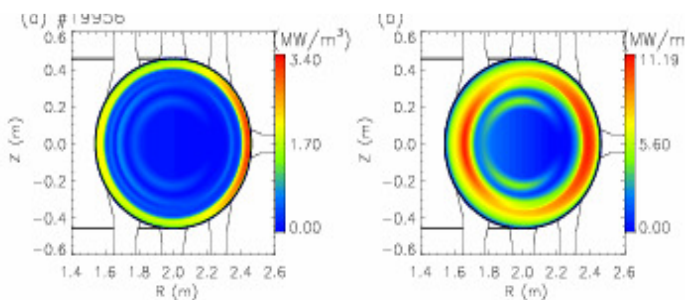


Fig. 4 Radiation pattern on the poloidal plane (a) when the plasma is not shrunk due to the  $m=0$  (b) in the shrinking region

reaching at the edge a value about twice than in the core. It is worth noting that the radial extension of the density peak is of the same order of the radiation. A possible explanation for this toroidal accumulation of density comes from the plasma flow measurements, discussed below.

It has to be recalled that the data reported here refer to discharges where a rotating perturbation was externally applied to rotate the  $m=0$  and allow the observation with all the

emissivity map, as obtained by the tomographic bolometry system, compared with the local displacement from the wall of the  $m=0$  perturbation  $\delta^0$  (fig. 2a, red curve). In the plot, the abscissa represents the toroidal angle of the diagnostic with respect to the instantaneous position of the LM ( $\Phi_{\text{lock}}$ ). Most of radiation is toroidally localized in a belt about  $30^\circ - 90^\circ$  wide, corresponding to the region where the LCFS deformation due to the  $m=0$  perturbation induces a shrinking of the plasma. The same toroidal asymmetry is not observed at lower densities, with  $n/n_G < 0.4$ .

An example of oxygen line intensity ratio behaviour is shown in fig. 2c. As the total radiation, the O VI (Li-like) and O IV (boron-like) line intensities increase at an angle displaced by  $\sim 100^\circ$  from the LM. This implies, rather than a strongly recombining plasma, a widening of the radial region at low temperature (20-40 eV) where these ions mainly emit. Measurements from Thomson scattering confirm this indication (fig. 3) [15].

On the poloidal plane, the radiative region at high density is nearly symmetric, and forms a quite broad belt (radial extension  $\sim 10$ -20 cm, 1/3 of the plasma radius, fig. 4b) where the plasma shrinks. In the other toroidal regions, the plasma radiation is poloidally asymmetric, peaked towards the outer part of the torus, where the PWI is stronger, and localized in a narrow layer ( $\sim 5$ cm, fig. 4a).

### 2.3 Density behaviour

In discharges approaching the Greenwald limit an increase of the electron density line-integrated signal is also observed, toroidally shifted by  $100^\circ$  with respect to the transit of the LM, i.e. where the plasma shrinks (fig. 5b, showing the inverted density profiles obtained from a multichord

interferometer as a function of the toroidal angle). The increased density is not the simple consequence of a local enhancement of the source, as the  $H_\alpha$  intensity, proportional to the neutrals entering the plasma, peaks in correspondence of the LM (fig.5a).

The increase of density corresponds to a radial profile externally peaked (see fig. 5b),

diagnostic systems. However, high density plasmas without rotating perturbation showed the same global behaviour and also in that cases radiating belts corresponding to plasma shrinking were observed.

### 3. THE ROLE OF THE EDGE FLOW AND TRANSPORT

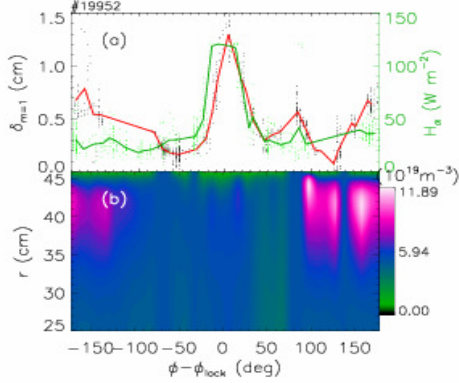


Fig. 5:  $H\alpha$  emissivity and  $m=1$  perturbation (a) and electron density radial profiles (b) vs. the toroidal angle

$T_i=T_e$ ), and has been found to be negligible. Therefore, taking into account that in a RFP at the edge  $B \sim B_\theta$ , the toroidal velocity can be considered as  $v_\phi \sim E_r/B_\theta$ , where the negative sign of  $v_\phi$  corresponds to an inward  $E_r$ . The  $E_r$  behaviour as a function of the electron density is plotted in fig. 6 for two currents. Data in the plot refer to the region where the LCFS does not intercept the wall, i.e. where plasma shrinks and radiating belts are observed. For each current,  $E_r$  decreases with density up to a sort of ‘saturation’ level, reached at  $n/n_G \sim 0.4$ , the same value above which the radiating belts are observed. The decrease of the electric field at high density can be associated to a decreased rate of Finite Larmor Radius (FLR) losses, due to the lower temperature and to the higher viscous effect associated to the charge exchange processes [19]. In the region where the magnetic field lines, intercepting the wall, directly hit against it, the local  $E_r$  depends on the loss rate of electron and ions, determined by the sign (inwards or outwards) of the radial magnetic field. In that region the sign of  $E_r$ , and therefore of  $v_\phi$ , is determined by the local  $B_r$ . Fig. 2a shows that when the  $\delta^0$  derivative becomes negative and the radial magnetic field is positive (outwards) [20], the toroidal velocity changes sign, while it reverts negative as  $B_r$  changes sign. The same behaviour is also shown

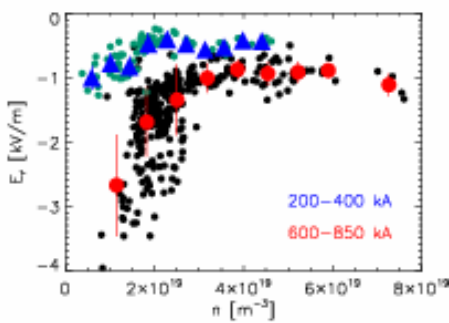


Fig. 6: Radial electric field vs density; the total density range has been divided in 10 intervals: red and blue points are the average over such intervals

The plasma toroidal velocity at the edge has been measured by a Gas Puffing Imaging (GPI) diagnostic as a function of the electron density [16]. In principle, this is not properly the plasma velocity, but the velocity of the density fluctuations evaluated from a cross correlation technique applied to the He I line emission. However, the fluctuation velocity has been found consistent with the  $\mathbf{E} \times \mathbf{B}$  drift obtained from the plasma potential gradient [17,18], and can therefore be identified with the plasma velocity writing  $\mathbf{v} \sim (\mathbf{E} \times \mathbf{B})/B^2$ . The diamagnetic term in the momentum balance equation  $E_r = (\nabla p_i)_r / (en_i) - (\mathbf{v} \times \mathbf{B})_r$  ( $p_i$  plasma pressure) has been experimentally determined at the edge from the  $T_e$  and  $n_e$  profiles obtained from the intensity ratio of He I lines (and assuming

by the velocity measured from the Doppler shift of a C III line, emitting from the plasma edge. The picture emerging from the results is that particles entering into the plasma are mainly produced in the region of LM (where the  $H_\alpha$  shows a strong increase) and are toroidally conveyed towards a stagnation point, displaced by  $\sim 100^\circ$  with respect to the LM and corresponding to the region where the  $m=0$  perturbation is associated to a shrinking of the plasma. There, at high density, particles accumulate, radiation increases and the plasma cools down. In RFX-mod at high density, smaller blobs are nested into larger ones, corresponding to more effective coherent structures with higher density [16]. Indeed,

also in Tokamaks the high density regimes are characterized by blobs at higher density [21]. Taking into account that a large part of transport, of the order of 50%, is due to blobs at  $n/n_G > 0.3$  [21,22], the density accumulation may be viewed as an accumulation of blobs with higher density. The effect is favoured by a turbulent diffusion coefficient  $D_p$  (representing the contribution to the total of the coherent structures) decreasing with  $n/n_G$ , as reported in [23] and showing no dependence on the toroidal angle. The diffusivity not related to blobs has been found to be well described as a Bohm-like diffusivity in RFX-mod. The edge electron temperature decreases with density [24], indicating that also the Bohm component of diffusivity is not expected to increase in the region of density accumulation. The question arises if a toroidal density gradient can be maintained against the radial diffusion. The radial diffusive flux  $D \partial n_{\text{edge}} / \partial r$ , evaluated on the basis of the diffusion coefficient experimentally determined for RFX-mod [25], is  $\approx 10^{22} \text{ m}^{-2} \text{ s}^{-1}$ , to be compared with a toroidal convective flux (that in the case of a RFP at the edge is a perpendicular flux)  $v_\phi n_{\text{edge}} \approx 10^{23} \text{ m}^{-2} \text{ s}^{-1}$ . Summarizing, the density accumulation in the region of the plasma shrinking can be due to the combined effect of the flow inversion originated by the edge radial field and of the edge transport dependence on density.

#### 4. – EFFECT OF THE MAGNETIC TOPOLOGY

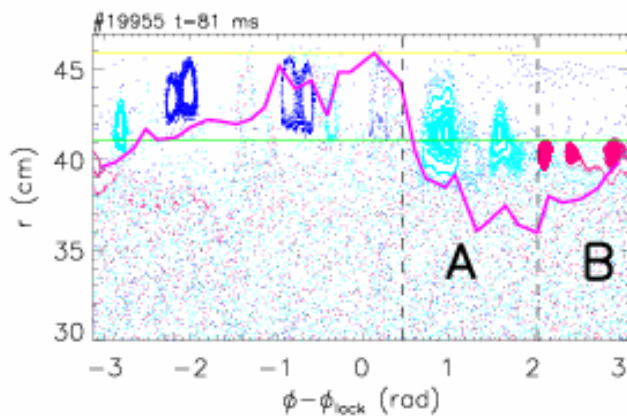


Fig.7 : Poincaré' plot of the magnetic topology at the edge. Green line: reversal surface; magenta line: toroidal flux function

The above discussion implies a strict link between the phenomenology at high density and the topology of the magnetic field, in particular of the  $m=0$  modes. To study this point, the Hamiltonian guiding center code Orbit [26] has been applied, using as input perturbation the eigenfunctions calculated as solutions of the Newcomb's equations for  $m = 0, 1$  and  $n = -1 - -24$  in toroidal geometry [27]. Fig.7 shows the resulting toroidal Poincaré' plot for a discharge with  $n/n_G = 0.8$ , at the time of the radiation peak. The toroidal field ripple  $\psi^0$  due to the  $m=0$  and the toroidal field reversal surface are also shown in the figure. A chain of  $m = 0$  islands is reconstructed, with the O-points aligned in the toroidal direction nearby the reversal radius. At  $\Phi < \Phi_{\text{lock}}$  the islands are pushed towards the wall, while islands at  $\Phi > \Phi_{\text{lock}}$  are shifted towards the axis. The region where  $\psi^0 < 0$ , which is the region where the plasma flow reverts its direction and radiation peaks, can be subdivided in two parts: one (A) where  $\partial \psi^0 / \partial \Phi < 0$  and  $B_r$  is positive, and the other one (B), where  $\partial \psi^0 / \partial \Phi > 0$  and  $B_r$  is negative. As a result of this modulation of the radial field, in region (A)  $m = 0$  islands are elongated radially up to 5cm and they can touch the wall, while in region (B) islands are compressed to  $\approx 1\text{cm}$  and are topologically well defined. As electrons at the first order follow field lines due to their smaller Larmor radius, they can be expected to flow along the border of islands in region (A), and to intercept the wall, while this does not happen in region (B). As a consequence, confirming the qualitative discussion given in sec. 3, the application of the Orbit code indicates that in (A) an outward electron flux can induce an inward electric field, which is elsewhere outward due to FLR effects, determining the flow inversion which is at the basis of radiation condensation. The key role of the  $m=0$  structure in influencing the plasma behaviour at high density is inferred from the operation of RFX-mod in the so-called ultra-low q (ULq) configuration

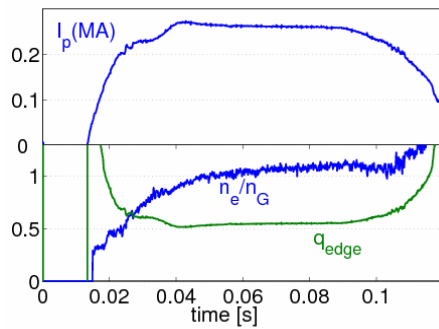


Fig. 8: plasma current (top), Greenwald fraction and edge safety factor (bottom) time evolution in a Ufq discharge

[28], a screw pinch characterized by a safety factor in the range  $0 < q < 1$ . In ULq plasmas a field reversal surface does not exist and the non linear coupling among the  $m=1$  modes is poor, with a consequent negligible amplitude of the  $m=0$ . Discharges with sustained plasma current and  $n/n_G$  exceeding 1 have been obtained, (fig. 8), suggesting that the achievement of RFP discharges with very low  $m=0$  perturbation could allow the overcoming of the Greenwald limit.

## 5. COMPARISON WITH TOKAMAKS AND STELLARATORS

The phenomenology observed in RFX-mod at high density shares a number of similarities with Tokamaks and Stellarators. The radiating belts observed in RFX-mod resemble the phenomenology of MARFES observed in Tokamaks and Stellarators [5,29,2,30], usually attributed to a thermal instability [31,32] (exchanging the poloidal and toroidal direction, as at the edge in RFPs the parallel transport is poloidal). However, the radiating belts observed in RFX-mod, that as MARFES are linked to an edge cooling of the plasma, have an impact on the plasma discharge different than in Tokamaks and Stellarators. A simple power balance has been calculated in the highly radiating region, comparing the dissipated power (radiation plus neutral excitation and ionization) with the heat flux to the same region from the radial direction and along the magnetic fields lines, calculated perpendicularly to the  $m=0$  perturbation as in [32]. The radiated power is evaluated assuming a concentration of 1% of the electron density for carbon and oxygen. This local estimate, though crude and qualitative, shows that, due to the high effective correlation length at the edge, where the toroidal field is very low, the contribution of the heat flow along the field lines is by about one order of magnitude lower than the perpendicular heat flux. When the electron temperature becomes lower than 25 eV, the dissipated energy exceeds the total heating flux, thus implying a further decrease of the temperature itself. This negative power balance is a local effect: differently from what observed in Stellarators [9], in RFX-mod the total radiated power remains well below the total heat power. However, the edge cooling does not lead to a disruptive instability. Indeed, if on the one hand processes of electron ejection and temperature collapse recovery are not observed as in Stellarators [2,9], on the other hand a soft landing of the plasma temperature and current is observed, rather than a disruption as it happens in Tokamaks, due to a shrinking of the current channel with the onset of an ( $m=2$ ,  $n=1$ ) instability. To interpret the impact of the radially localized radiative process on the global plasma performance, a 1-dim transport model has been applied, that self-consistently evolves the MHD fields and includes part of the RITM code [34] for the evaluation of the neutral and impurity related terms. The code solves the equation for the safety factor  $q(r,t)$  assuming an Ohm's law with a dynamo term and a Spitzer's like resistivity, together with the main gas transport equations. In Fig. 9 the effect of an increase of the density is shown. Following a forced linear increase of the Hydrogen influx (a), the density increases as a whole by a factor about 3 reaching values close to the Greenwald density and turning into a slightly hollow shape. The density increase leads to a decrease of the temperature (b), as experimentally observed and also to a current decrease (c). This effect is due to the freezing of the dynamo at the beginning of the particle influx: the plasma current is no longer sustained against the increased resistivity, resulting in a soft landing of the discharge. In other words, to sustain a constant plasma current, a great enhancement of the dynamo field would be required. It is worth noting that at the end of the density injection the volume integrated

radiation power turns out to be  $\sim 10\text{-}15\%$  of the ohmic input power, consistently with the experimental global power balance.

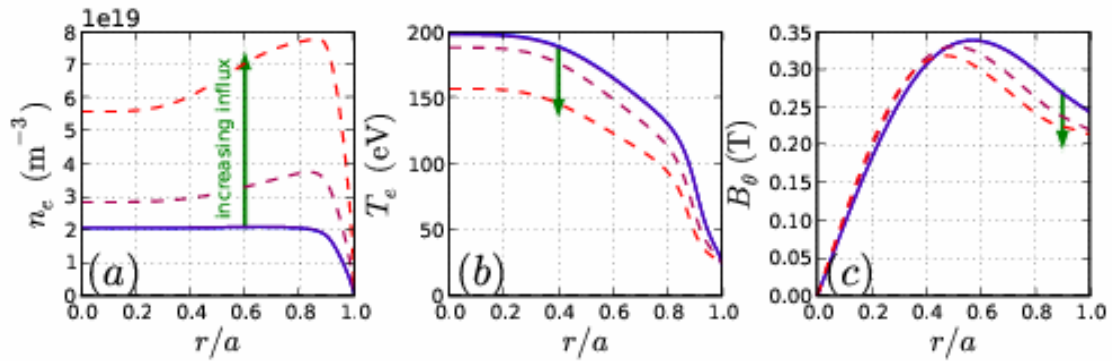


Fig. 9: Density (a), temperature (b) and poloidal field (c) profiles behaviour as obtained from the 1-dim model with time increasing particle

## 6. CONCLUSION

The phenomenology observed in RFX-mod high density plasmas can be summarized as follows: when density approaches the Greenwald value, a poloidally symmetric radiation belt develops toroidally localized, with a corresponding edge accumulation of density. The proposed interpretation is based on a combined effect of the toroidal flow inversion occurring where the magnetic field lines intercept the wall and of a decreased diffusivity at high density. A strict relation has been observed between radiation and magnetic topology: the radiating belt is observed where the plasma is shrunk due to the  $m=0$  perturbation. The importance of the  $m=0$  structure is confirmed by discharges in the ULq configuration, where it is greatly reduced and density can exceed the Greenwald value.

The radiating belt may be assimilated to the phenomenology of MARFES, observed in Tokamaks and Stellarators. In RFPs also it corresponds to a progressive cooling down of the plasma edge, radially extending towards the plasma core and with a dissipation locally exceeding the total heat flux. However, in RFPs the onset of this thermal instability does not end disruptively, but corresponds to a soft landing of the plasma discharge, associated to a dynamo incapable to sustain the current with the increased resistivity.

The open issue remains of the sustainment of a steady state high current RFP discharge at high density, in particular in the highly performing QSH regime. The results discussed in the paper suggest that a possible way relies on a strong reduction of the  $m=0$  perturbation, which is naturally achieved in QSH. At the same time, the operation at higher density can be favoured by a better control of the wall conditioning and recycling reduction, (for example applying techniques such as wall lithization), with a more efficient core plasma fuelling (pellets). Experiments on these directions are ongoing.

**Acknowledgements:** This work was supported by the European Communities under the contract of Association between EURATOM/ENEA.

## References:

- [1] Greenwald M., "Density limits in toroidal plasmas", Plasma Phys. Contr. Fus. 44 (2002) R27-R80
- [2] Wobig H., "On radiative density limits and anomalous transport in stellarators", Plasma Phys. Contr. Fus. 42 (2000) 931
- [3] Tokar M.Z., Kelly F.A., Loozen X. "Role of the thermal instabilities and anomalous transport in threshold of detachment and multifaceted asymmetric radiation from the edge (MARFE)", Phys. Plasmas 12 (2005) 052510

- [4] Valisa M. et al., “The Greenwald density limit in the Reversed Field Pinch”, Proc. 20th IAEA Fusion Energy Conference, Vilamoura, Portugal (IAEA, Vienna 2004) vol. IAEA-CN-116, EX/P4-13
- [5] Valisa M. et al., “Edge transport properties of RFX-mod approaching the Greenwald density limit”, Proc. 21st IAEA Fusion Energy Conference, Chengdu, China (IAEA, Vienna 2006) vol. IAEA-CN-149, EX/P3-17
- [6] Wyman M.D. et al., “Density control and limit(s) in MST”, Proc. Bull. 49th APS meeting, (2007)
- [7] Brower D.L. et al., “Confinement degradation and enhanced microturbulence as long-time precursors to high-density-limit tokamak disruptions”, Phys. Rev. Lett. 67 (1991) 200
- [8] De Vries P.C. et al., “Influence of Recycling on the Density Limit in TEXTOR-94”, Phys. Rev. Lett. 80 (1998) 3519
- [9] Giannone L. et al., “Physics of the density limit in the W7-AS stellarator”, Plasma Phys. Contr. Fus. 42 (2000) 603
- [10] Sudo S. et al., “Scalings of energy confinement and density limit in stellarator/heliotron devices”, Nucl. Fusion 30 (1990) 11
- [11] Paccagnella R. et al., “Active-Feedback Control of the Magnetic Boundary for Magnetohydrodynamic Stabilization of a Fusion Plasma”, Phys. Rev. Lett. 97 (2006) 075001
- [12] Marrelli L., Zanca P., Martin P., Martini S. and Murari A., “Edge localised asymmetric radiative phenomena in RFX”, J. Nucl. Mater. 266-269 (1999) 877
- [13] Valisa M. et al., “High current regimes in RFX-mod”, Plasma Phys. Contr. Fus., to be published in October 2008 (2008)
- [14] Martini S. and the RFX team, “Active MHD control at high currents in RFX-mod” Nucl. Fus. 47 (2007) 783
- [15] Alfier A., Pasqualotto R., “New Thomson scattering diagnostic on RFX-mod”, Rev. Sci. Instrum. 78 (2007) 013505
- [16] Scarin P. et al., “Edge turbulence scaling in RFX-mod as measured using GPI diagnostic” 18th PSI Conf. (Toledo, Spain 2008) to be published in Jour. Nucl. Mat.
- [17] Yu J.H. et al., “Examination of the velocity time-delay-estimation technique” J. Nucl. Mat. 363-365 (2007) 728
- [18] Antoni V. et al., “Anomalous particle transport and flow shear in the edge region of a RFP”, J. Nucl. Mat. 313-316 (2003) 972
- [19] Bartiromo R., “Plasma rotation and finite Larmor radius losses in a reversed field pinch”, Phys. of Plasmas 5 (1998) 3342
- [20] Zanca P. and Martini S., “ $m = 0$  perturbations of the magnetic surfaces in an RFP”, Plasma Phys. Contr. Fus. 43 (2001) 121
- [21] Boedo J.A. et al., “Transport by intermittency in the boundary of the DIII-D tokamak”, Phys. Plasmas 10 (2003) 1670
- [22] Spolaore M. et al., “Vortex-induced diffusivity in Reversed Field Pinch Plasmas”, Phys. Rev. Lett. 93 (2004) 215003
- [23] Martines E. et al., “Transport mechanism in the outer region of RFX-mod”, this conference, paper EX/P5-26
- [24] Carraro L. et al., “Edge temperature and density measurements with a thermal helium beam in the RFX reversed field pinch”, Plasma Phys. Contr. Fusion 42 (2000) 1
- [25] Innocente P., Alfier A., Carraro L., Lorenzini R., Pasqualotto R., Terranova D. and the RFX team, “Transport and confinement studies in the RFX-mod reversed-field pinch experiment”, Nucl. Fus. 47 (2007) 1092
- [26] White R.B. and Chance M.S., “Hamiltonian guiding center drift orbit calculation for plasmas of arbitrary cross section”, Phys. Fluids 27 (1984) 2455
- [27] Spizzo G. et al., “Transport Barrier inside the Reversal Surface in the Chaotic Regime of the Reversed-Field Pinch”, Phys. Rev. Lett. 96 (2006) 025001
- [28] Bonfiglio D., Cappello S., Piovan R., Zanutto L., Zuin M., “3d nonlinear MHD simulations of ultra-low  $q$  plasmas”, accepted for publication in Nucl. Fus.
- [29] Lorenzini R., et al., “Toroidally asymmetric particle transport caused by phase-locking of MHD modes in RFX-mod” Nucl. Fus. 47 (2007) 1468
- [30] Lipschultz B., “Review of Marfe phenomena in Tokamaks”, J. Nucl. Mat. 145-147 (1987) 15
- [31] DePloey A. et al., “Marfes: a magnetohydrodynamic stability study of two-dimensional tokamak equilibria”, Plasma Phys. Contr. Fus. 39 (1997) 423
- [32] Tokar M.Z. et al., “Localized recycling as a trigger of MARFE”, J. Nucl. Mat. 266-269 (1999) 958
- [33] Carraro L. et al., “The role of mode-locking in the fast termination of high density and high current RFX discharges”, Proc. 28th EPS Conf. on Contr. Fus. and Plasma Phys., Funchal, Portugal, (2001), vol. 25A, 1545
- [34] Tokar M. Z., “Modelling of detachment in a limiter tokamak as a nonlinear phenomenon caused by impurity radiation”, Plasma Phys. Control. Fusion 36 (1994) 18